7-2008

Repair of Full-scale Timber Bridge Chord members by Shear Spiking

Travis A. Burgers

Richard M. Gutkowski

Jeno Balogh

Donald W. Radford

REPAIR OF FULL-SCALE TIMBER BRIDGE CHORD MEMBERS BY SHEAR SPIKING

Travis A. Burgers [1], Richard M. Gutkowski [2], Jeno Balolgh [3], Donald W. Radford [4]
1 Doctoral Student, Dept. of Mechanical Eng., University of Wisconsin, Madison, WI
2 Prof., Dept. of Civil Eng. Colorado State University, Fort Collins, CO 80523
3 Asst. Prof., Civil Eng. Technology, Metropolitan State College of Denver, Denver, CO 80217
4 Prof., Dept. of Mechanical Eng., Colorado State University, Ft. Collins, CO 80523

Abstract

The addition of vertically-oriented shear spikes (fiberglass reinforced polymer rods) was shown to increase the effective stiffness of the stringers of a full-scale timber bridge chord specimen. Results found from the flexural load testing of a full-scale timber bridge chord laboratory specimen are presented. Reinforcement was provided with 19 mm diameter shear spikes bonded to the wood by an epoxy resin. The bridge chord specimen was intentionally damaged to simulate degradation. Shear spikes were then installed from the top of the member into pre-drilled holes to provide horizontal shear resistance and to improve the flexural effective stiffness. Results from the testing showed that with the insertion of five sets of shear spikes the average flexural effective stiffness recovered in the four stringers of the chord was 91.6%.

CE Database subject headings: Rehabilitation; Bridges, wood; Stiffness; Fiber reinforced materials; Deterioration.

Introduction

Numerous timber trestle railroad bridges built before World War II are nearing the end of their service lives because of deterioration, fatigue, or both. Advances made in the railroad industry have led to loads which exceed those used by the original bridge designers. Many of these bridges are theoretically no longer able to support the contemporary design loads, much less the 20% axle load increase anticipated in future railroad traffic (Oomen and Sweeney 1996). Consequently extensive research on methods to strengthen timber bridges has ensued. Some of this research includes replacing deteriorated members (Uppal and Otter 1998), wrapping members with fiberglass (GangaRao, Sonti, and Superfesky 1996) or carbon fiber sheets (Johns & Lacroix 2000), and installing fiberglass reinforced polymer (FRP) rods longitudinally near the tension or compression faces (Gentile, Svecova, and Rizkalla 2002). All these methods are very expensive. A process termed “Z-spiking” offers a potential alternative to these methods.

Z-spiking consists of installing vertically-oriented FRP pultruded rods in timber members to stiffen and strengthen them.

The concept of Z-spiking comes from the aerospace industry (Cox 1999, Steves & Fleck (1999). The advantages of Z-spiking are high performance, low cost, and compatibility of material properties with the wood. This technique was the basis for the research studies described herein.

Related Research

Bulleit (1984) summarized past studies on methods to reinforce beams, plywood, and particleboard. Some examples included reinforcing wood with post-tensioned, high strength steel strands in their tension zone (Bohannan 1962), placing aluminum sheeting vertically between wood laminates (Sliker 1962), using steel rods in grooves (Lantos 1964), and bonding steel plates were bonded to the tension face of laminated beams (Peterson 1965).

GangaRao, Sonti, and Superfesky (1996) examined timber beams wrapped with a glass fiber reinforced composite (GFRP). The GFRP wrap increased the modulus of elasticity by 15–41% and the modulus of rupture by 14–31%. The ductility of the beams was also increased. Davalos, Zipfel, and Qiao (1999) utilized a finite element (FE) model to compute how to minimize the volume of GRFP reinforcement needed in wrapping timber beams. The study showed that the wrap need not be uniformly placed over the length of the beam. Load tests showed that the linear load versus deflection responses of the wood-GFRP wrap samples could be accurately predicted. Gentile, Svecova, and Rizkalla (2002) conducted experimental research on creosote-treated, Douglas fir solid sawn timber beams. Two spans were studied, 4.3 m and 10.4 m. Grooves were cut in either the side faces or the bottom face. GFRP rods were placed in the grooves using epoxy. The diameter of the rods was 5 mm for the shorter spans, and either 10 or 13 mm for the longer span. The longer spans were inserted at 1-m intervals to hold the rods in place during the application of epoxy. The beams were load tested to find differences in flexural stiffness and ultimate flexural strength. The flexural stiffness increased by 5–7% and ultimate flexural strength increased by 18–46%. The failure mode was a ductile compressive failure in the compression zone of the timber.

Barbero, Davalos, and Munipalle (1994) conducted shear tests to measure the ultimate strength of three adhesives for various interface combinations: sapwood-sapwood, heartwood-heartwood, sapwood-vinylester, sapwood-polyester, heartwood-vinylester, and heartwood-polyester. Each interface combination was bonded by either resorcinol formaldehyde, emulsion Isocyanate, or epoxy. Twenty wet and 20 dry samples were tested. The ratio of shear strength of the wet specimens compared to dry specimens was 0.53. An FE model predicted a similar ratio.

Davalos, Qiao, and Trimble (2000) examined long-term performance and delamination behavior of wood-FRP composites. A high number of variables including types of adhesive, bonded materials, and coupling agents were considered. It was determined that a standard test could assess the effect of bonding parameters, but performance evaluation tests were not sufficient to predict the effects of temperature, moisture, and service load conditions on delamination. Later, Davalos, Qiao, and Trimble (2000) evaluated fracture response of wood laminates. They found that a contoured double-cantilever beam specimen can effectively be used to find fracture toughness values for Mode I failures.

Radford et al. (2000–2003) examined the effect of adding Z-spikes to dimension lumber. First, groups of two layered, nominal “2x2”s (actual dimensions 38 x 38 mm) were joined with 12 pairs of 3 mm diameter shear spikes bonded with epoxy resin. The spacing along the length of the members was 76 mm. The average increase in flexural stiffness relative to the unattached, layered 2x2s was 160%. Next, individual normal “2x4s” (actual dimensions 38 x 89 mm) were sawn longitudinally along the centroidal axis from each end to within 51 mm of the center (midspan). Pairs of shear spikes were inserted incrementally so that there were six sets of two on each side of the centerline. Load tests showed that the flexural stiffness essentially returned to the level of the undamaged 2x4.

Schilling et al. (2004) used 13 mm diameter FRP shear spikes to reinforce deteriorated railroad crossties. The intent was to extend Radford et al's (2000–2003) work to larger wood members. Thirty-five Douglas-fir crossties were sorted by "appearance" and "flexural stiffness." The appearance rating incorporated the size of the horizontal cracks and the number of longitudinal faces that showed obvious deterioration. The flexural stiffness rating ranked the crossties based on the measured values determined by load testing. In each sorting method, the crossties were rated in one of the following categories: high, medium, or low. Then the ratings from both methods were combined to rate the crossties as either high, medium-high, medium, medium-low, or low. Ten low quality and ten medium-high quality crossties were selected for Z-spiking. Shear spikes were installed in a procedure similar to that used by Radford et al. (2000–2003). Five pairs of spikes were incrementally installed symmetrically on each side of about the center line of the crosstie, starting from the ends of the beam and working toward the center. An entire row was installed in one day. The epoxy was allowed to cure for two days. For the low quality group, the average increase in flexural stiffness was 65.8%. A 29 kN ramp loading was applied at midspan of the crosstie, before and after the shear spikes were inserted. The flexural stiffness, EI, of the crossties was measured from the simple beam bending equation. For the medium-high quality group, the average increase was 51.0% flexural stiffness. The approximate total cost (labor and materials) of the repair procedure was $67.49 per crosstie. The labor cost for a five-person crew to replace a bridge stringer would be approximately $2400 per stringer. The researchers reported that by using the shear spike method, it would cost approximately $387 to reinforce an individual stringer.

Objective of the Study

The objective of the study described herein was to examine the effectiveness of using Z-spikes to reinforce a chord of a timber trestle railroad bridge. The hypothesis was that there would be a significant improvement in the flexural effective stiffness of a damaged, full-scale open-deck timber trestle bridge chord test specimen when repaired with vertically-oriented shear spikes.

Experimental Test Setup

The laboratory test specimen was a full-scale partial chord of an open-deck timber trestle railroad bridge. A train load is essentially equally shared by the two chords, so a single chord will get half of the train load. Thus, testing a single chord is the idealized case for imposed train loading.

Because the objective was to observe the effects of Z-spiking on the stiffness of large members, it was decided that the stringers would be the only timber members used in the test specimen. This isolated the primary issue from side effects of other components. Removal of the steel rails and crossties also reduced the required test load.

A three-span, four stringer bridge chord was constructed as shown in Figure 1. The materials were donated by the Association of American Railroads and had been used in a previous research project (Doyle et al. 2000). In that project, the specimen was essentially a full-scale replication of a complete chord of an actual bridge previously tested in the field (Gutkowski et al. 1999–2002). Test loads used then were well below the ultimate strength of the stringers, thus they were intact. However, for the purposes of the research described herein, any damage that might have been inflicted would be advantageous.

Figure 1: Photograph of Full-Scale Specimen

The bridge chord specimen was comprised of four two-span continuous members and four single-span members. As shown in Figure 2, each span was 4.01 m, center to center of the supports, which was slightly less than the typical 4.3–4.6 m. The shorter spans were necessitated by space restrictions. The cross sectional dimensions of each stringer varied slightly, but they were all approximately 200 mm wide and 400 mm deep. The single-span members were placed in the end spans and were alternated with the two-span continuous stringers, which is standard in construction (American Railway Engineering Association, (1995)). All the stringers were tied down at the supports to prevent uplift. Steel tie rods (five per span) were placed to laterally interconnect the four stringers and 50 mm spacers were used to keep the beams separated.

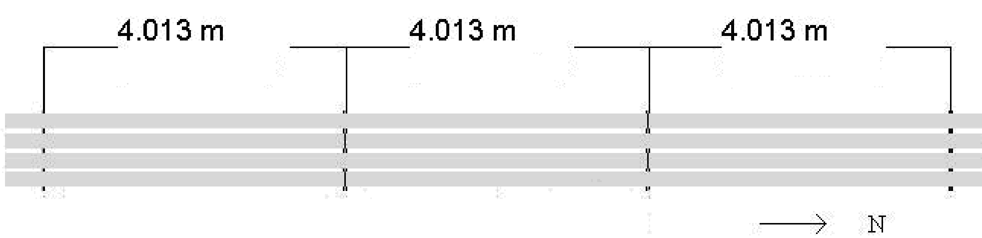

Figure 2: Plan View Schematic of Spans.

Damaging the Timber Stringers

The ultimate objective of the study was to apply Z-spiking to the members of timber bridges. The stringers used were in good physical condition. A bridge member in good condition would not need to be rehabilitated. For this reason, intentional damage was inflicted on the stringers.

The location of the controlled damage was determined by a computer model using the commercial structural analysis software package, Axis VM (InterCad 2003). Details were provided by Burgers et al. (2005).

The south half of the center span of the bridge chord was intentionally damaged by horizontally cutting the beams at mid-depth. The cut was made from the south interior support towards the loading point on only the center span. This was first attempted using a two-man hand saw, resulting in a cut of approximately 200 mm length in 8 hours. Thus, a chainsaw was then used to inflict further damage, albeit creating a much more severe width of cut than originally intended. The cut was shimmed so the gap would not close when load was applied to the specimen. The chainsaw damage and shimming is shown in Figure 3. The chainsaw was used on each side of the specimen to cut two stringers at a time, but the blade did not reach the inner 50 mm of the inner two stringers. The rest of the damage to the two inner stringers was done by loading the bridge and letting the load propagate the crack. In doing this, a crack was initiated at the end of the cut and extended into the center third of the span, between the two load points. The north half of the center span of the bridge chord was then cut using the chainsaw, but the remaining uncut segments of the two interior stringers were cut using the two-man wood handsaw.

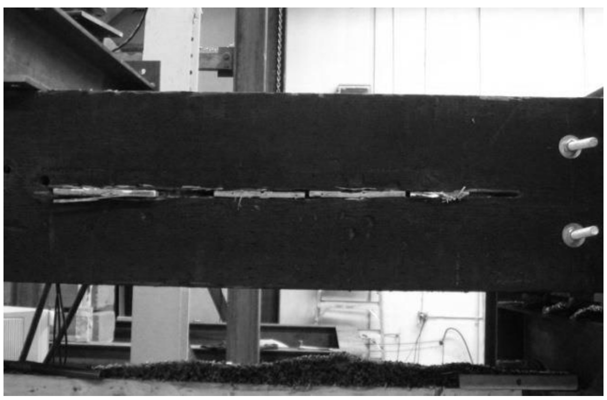
Figure 3: Shimmed Chainsaw Damage

Z-spike Installation

The Z-spikes used are shown in Figure 4. Z-spikes were each cut from a 1.50 m long base rod stock obtained from Liberty Pultrusions. Each rod was cut to a length of 406 mm, the same as the depth of the timbers, leaving approximately 13 mm protruding from the top face of the timber upon installation. An angle grinder was used to bevel a point out of the last 25 mm of the leading edge of the rod. This reduced the force required to drive the rods and avoided a blunt end of the rod scraping the epoxy mix off the sides of the hole during installation.

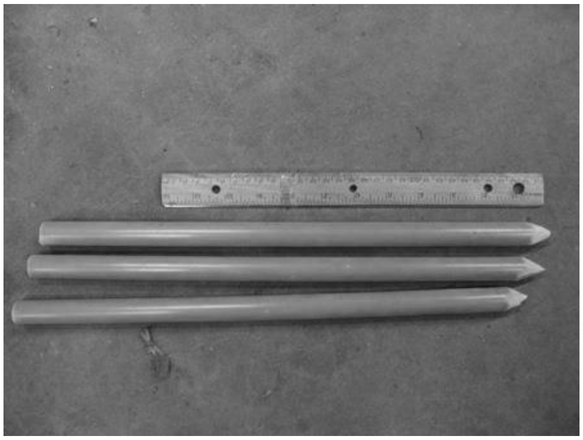

Figure 4: Z-spikes: 19 mm diameter, 406 mm length

After an initial load test on the intentionally damaged specimen, pairs of Z-spikes were incrementally installed in the south half of the center span of the test specimen. In each increment the two spikes were located at the third points of the stringer width.

The progress of the damage and repair of the south half of the center span was measured 11 times. Short labels are given before the description and are used in the subsequent figures.

1) No damage – The specimen was tested before any damage.
2) 8 inch cut (before crack) – A 203 mm cut was made that extended from 483 to 686 mm from the south support. During the load test to measure the effective stiffness of the 203 mm (8 inch) cut, there was a loud crack.
3) 8 inch cut (after crack) – Upon inspection of the specimen, it was evident that visible damage had occurred, particularly in the two beams on the east side, so the specimen was retested with the 203 mm cut.
4) Full cut completed – The cut was completed; it extended from 203 mm (8 inches) to 1320 mm from the south support.
5) Z-spikes in end – One set of Z-spikes was placed at 305 mm from the south support.
6) Repaired center beams (south) – Then, the region between the two distributor plates was repaired. First the south half was repaired. In the repair of the south half, four sets of Z-spikes were placed at approximate 127 mm spacings from the midspan to the south distributor beam at 51, 216, 343 and 457 mm from the midspan.
7) Repaired center beams (north) – Then the north half of the region between the distributor beams was repaired. Three sets of Z-spikes were placed at approximate 127 mm spacings from the midspan towards the north distributor beam.
8) 1st set of Z-spikes – Next, the Z-spikes were added to the cut. The first set of Z-spikes was placed 813 mm from the south support.
9) 2nd set of Z-spikes – The second set of Z-spikes was placed 457 mm from the support.
10) 3rd set of Z-spikes – The third set of Z-spikes was placed at 1220 mm from the support.
11) Repaired center beams (south 2) – Next, the region between the two distributor beams was further repaired. A total of three sets of Z-spikes were added at 140, 279, and 393 mm from the midspan between the four sets already in place between the midspan and the south distributor beam. Two sets were also added to continue the approximate 127 mm spacing under the south distributor beam at 508 and 610 mm from the midspan. The repair locations between the distributor beams are shown in Figure 5. In the figure, the

dimensions above on the south half label the Z-spikes used in the first repair. The dimensions on the north half label the Z-spikes used in the second repair. The dimensions below on the south half label the Z-spikes used in the third repair.

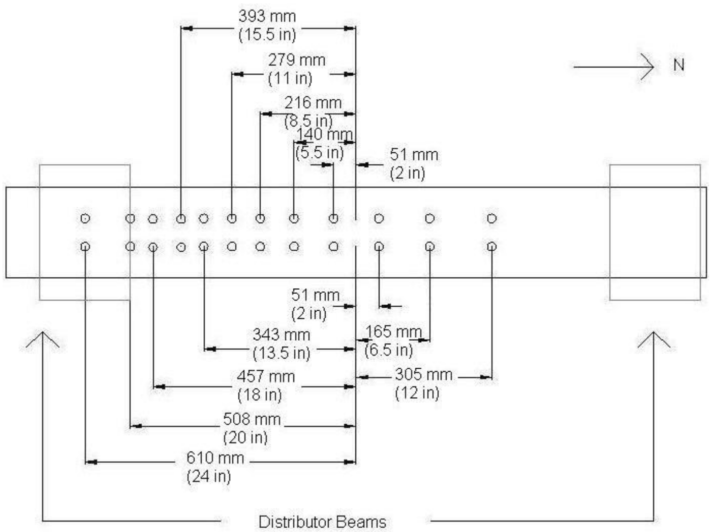

Figure 5: Z-spike Center Repair

Z-spikes in the north half of center span were placed in the following order (the locations are shown in Figure 6):

1) at the center point of the damage, 787 mm from the support.
2) at the three-quarters point of the damage, 1050 mm from the support.
3) at the quarter point of the damage, 521 mm from the support.
4) at the eighth point of the damage, 387 mm from the support.
5) at the three-eights point of the damage, 654 mm from the support.

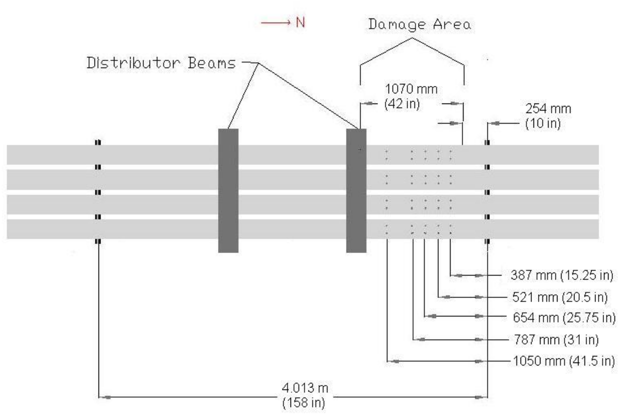

Figure 6: Plan View of Z-Spike Locations

The Z-spikes were added at the center of the damage first because that was the best location if only one pair was to be used, based on a computer model (Burgers et al. (2005)). The second and third Z-spikes were added at the three-quarter and one-quarter points of the damage because these were the best locations if three were to be used. The fourth and the fifth spikes were added closer to the support because the rods were more effective closer to the support than the load.

Each Z-spike was inserted in a manner similar to that of Schilling et al. (2004). First, a pilot hole was drilled to 330 mm with a 13 mm diameter bit. Next, a 19 mm diameter auger bit was used to enlarge the hole to a depth of 394 mm. That hole did not penetrate the member so that when the epoxy was placed it would remain in the hole. Finally, a 21 mm diameter bit was used to ream the upper 100 mm of the hole to increase the ease of installation.

The epoxy used for bonding the FRP rods to the wood was a three-part mixture made from ingredients obtained from the supplier, West Systems. The 105-epoxy resin was mixed with the 206-hardener in a 5:1 resin to hardener ratio. Silica thickener was added to increase the viscosity to approximately the consistency of baker's frosting. This prevented the mixture from freely flowing to the bottom of the holes during insertion. The exact amount of silica thickener was not measured as it was added in stages and the final consistency was determined by visual inspection. The resin-hardener-silica combination has been shown to bond well to both the FRP and the wood. The pot life is 20–25 minutes with a solid state time of 10–15 hours. The maximum strength of the final cure is attained in 1–4 days. These times are highly dependent on the room temperature, with lower temperatures resulting in longer cure times. During application of the epoxy mixture in this research, the temperature was held near room temperature, which was within the 15–32 ºC (60–90 ºF) manufacturer specification. Approximately 60 mL of epoxy was used for each Z-spike. The epoxy was poured into the hole and the Z-spike was pounded in with a wooden block. An entire row of Z-spikes was installed in one work day and the epoxy was allowed to cure for two days before the load testing was performed.

Loading

Two hydraulic actuators were used to apply a load at each one-third point along the longitudinal centerline of the center span (see Figure 7). A lateral distributor beam was placed below each actuator cylinder to distribute the load to the four stringers.

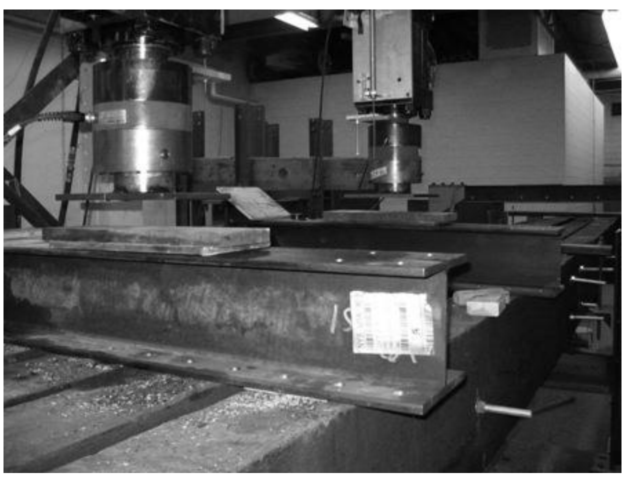

Figure 7: Actuators and Distributor Beams

Each actuator was to be loaded to 311 kN to intentionally fracture the 51 mm of the width of the inner stringers that the chainsaw could not cut. Because of the unintentional damage caused, the subsequent maximum load was reduced to 156 kN per actuator. After the north half of the center span was intentionally damaged using the chainsaw, the maximum load was further reduced to 111 kN, but during the loading, a loud cracking noise was heard. After the cracking noise occurred, the specimen was loaded again. It was deduced that it had not been further damaged because the load-displacement curves from before and after the cracking noise matched. Nonetheless, the subsequent loadings were reduced to 67 kN per actuator.

Vertical deflections of the test specimen were measured using Celesco string potentiometers. These were attached to the underside of each stringer at the midspan of each span, in the center of the width of each stringer.

Material Properties

The stringers were solid sawn, creosote pressure-treated Douglas-fir timbers. The stringer configuration is shown in Figure 2 and the measured dimensions of each member are listed in Table 1.

Table 1: Stringer Dimensions and Properties

Beam	b (mm)	h (mm)	MOE (MPa)
1	203	406	1.30E+04
2	210	406	1.43E+04
3	197	406	8.60E+03
4	210	400	1.06E+04
5	191	406	9.90E+03
6	197	419	7.38E+03
7	197	413	9.91E+03
8	200	419	9.70E+03

Four-point load tests were used to measure the MOE of each stringer before the bridge chord specimen was created and the damage inflicted. The calculated MOE values are shown in Table 1.

Based on manufacturer literature, the average ultimate tensile strength and longitudinal compressive strength of the rods was 483 and 276 MPa, respectively. The average transverse compressive strength and flexural strength at room temperature was 138 MPa and 483 MPa, respectively. The average flexural modulus of elasticity was 2.1 x 10^4 MPa. Other technical data are included in the manufacture literature (Liberty Pultrusions 2000).

Results

Evaluation Methodology

Results of the load testing were used to determine the effective stiffness of each member in the center span and the effectiveness in each span. The effective stiffness (ST) in kN-m^2 was calculated by substituting the measured span length (*l*) in meters and the slope ($\delta P/\delta\Delta$) of the corresponding measured load-deflection plot in kN/m into Equation 1. This equation was derived for a two-span continuous beam with the load (P) applied at the third points of one span and the deflection (Δ) measured at midspan of the loaded span. The constant ¼ was used because the load used in the slope ($\delta P/\delta\Delta$) was the total load applied to the four stringers.

$$ST = \frac{1}{4}\left(\frac{\delta P}{\delta \Delta}\right)\left(\frac{l^3}{2692/65}\right) \qquad \text{(Equation 1)}$$

The efficiency of the Z-spikes is given by Equation 2, as taken from Pault (1977).

$$Efficiency\ \ of\ \ repair_j = \frac{ST_j - ST_i}{ST_k - ST_i} \times 100\ \% \qquad \text{(Equation 2)}$$

where ST_i , ST_j , and ST_k are effective stiffnesses at chosen stages of load testing. A common use of this equation would assign ST_i to the minimum measured effective stiffness (e.g. the original full damage state), ST_k to be the maximum measured effective stiffness (e.g. the fully repaired state), and ST_j to be an intermediate effective stiffness (e.g. a partially repaired state). In this case, Equation 2 defines the efficiency of the intermediate ST (ST_j) relative to the minimum (ST_i) and maximum (ST_k) ST values.

Using the center span of the west stringer as an example, the undamaged north half had a ST of 1.03×10^4 kN-m^2 (ST_k) the completely damaged ST was 8.54×10^3 kN-m^2 (ST_i) and the ST when five sets of Z-spikes were added was 1.02×10^4 kN-m^2 (ST_j). Substituting these values into Equation 2, the efficiency of the five sets of Z-spikes relative to the minimum and maximum ST values is:

$$\frac{10.2 - 8.54}{10.3 - 8.54} \times 100\ \% \quad = 89.5\,\%$$

In other words, five sets of Z-spikes recovered 89.5% of the stiffness lost due to creating the original fully damaged state.

In each of the three spans, each of the four stringers was given a set of labels for various segments of the bridge chord specimen, as shown in Figure 8.

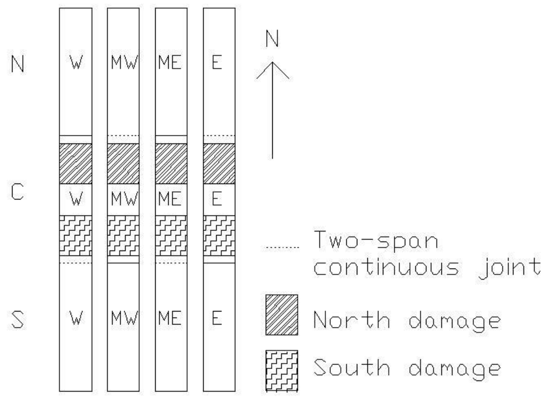

Figure 8: Stringer Labels

Damage/Repair to South End

The effective stiffness and efficiency were calculated at the 11 damage/repair increments provided earlier in the paper. For the damage/repair in the south half of the beam, load test data were not available to distinguish how much ST changed due to the cut and due to the unexpected damage (cracking of the beam).

The patterns of changing ST of the center span due to the south end damage/repair are shown graphically in Figure 9. The load-deflection data used to calculate the effective stiffness for the south end damage/repair can be found in Burgers et al. (2005).

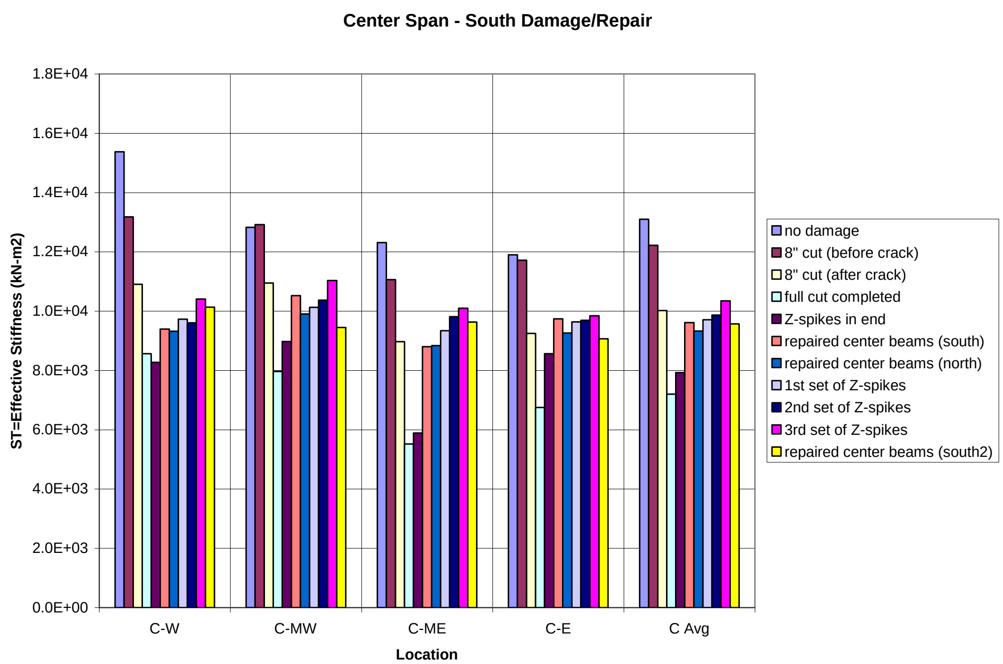

Figure 9: Effective stiffness of the center span due to south damage/repair

The decreases in efficiency caused by the progression of damage are shown in Figure 10. The "no damage" state was used as ST_k and the "full cut completed" state was used as ST_i in calculating efficiency from Equation 2. The efficiency equation and states ST_i, ST_j, and ST_k were used, but the definition of efficiency does not hold, since the data shown was for progression of damage and not repair. Instead the figure shows how the effective stiffness decreased with increasing damage. It was evident that the cut reduced the effective stiffness of each stringer.

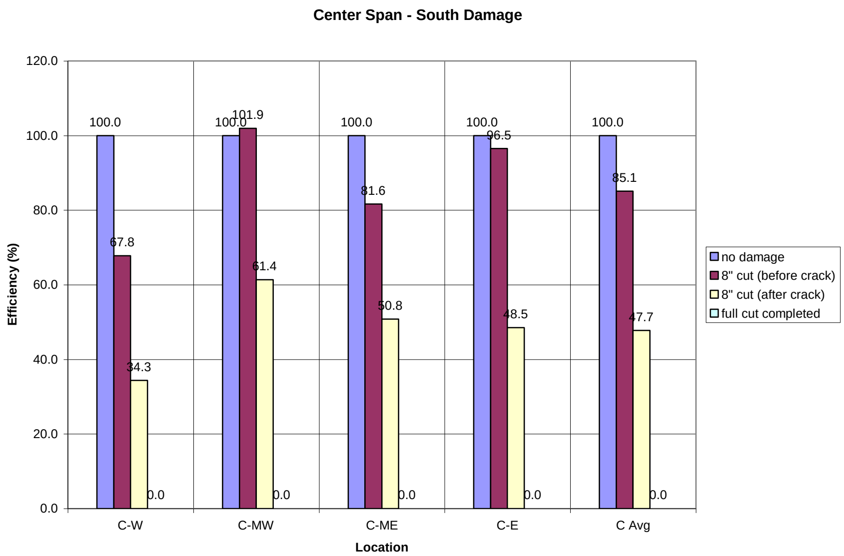

Figure 10: Efficiencies of the center span due to south end damage
(ST_i = "full cut completed" and ST_k = "no damage")

The efficiencies of the center repair progression are shown in Figure 11. The "repaired center beams (north)" state was used as ST_k and the "full cut completed" state was used as ST_i in calculating efficiency from Equation 2. It was evident that the installation of Z-spikes in the middle of the center span increased the effective stiffness. The effective stiffness was higher after the south half of the center of the span was repaired than when both the south and the north halves were repaired. A possible explanation is that the loss of the "sound" timber due to the drilling of the holes for the Z-spikes had more of a negative effect than positive effect of the insertion of the Z-spikes. Note that in the west stringer, the efficiency decreased with the addition of the shear spikes near the end of the damage. This interesting phenomenon was also observed in previous studies, i.e. Radford et al. (2000) and Schilling et al. (2004).

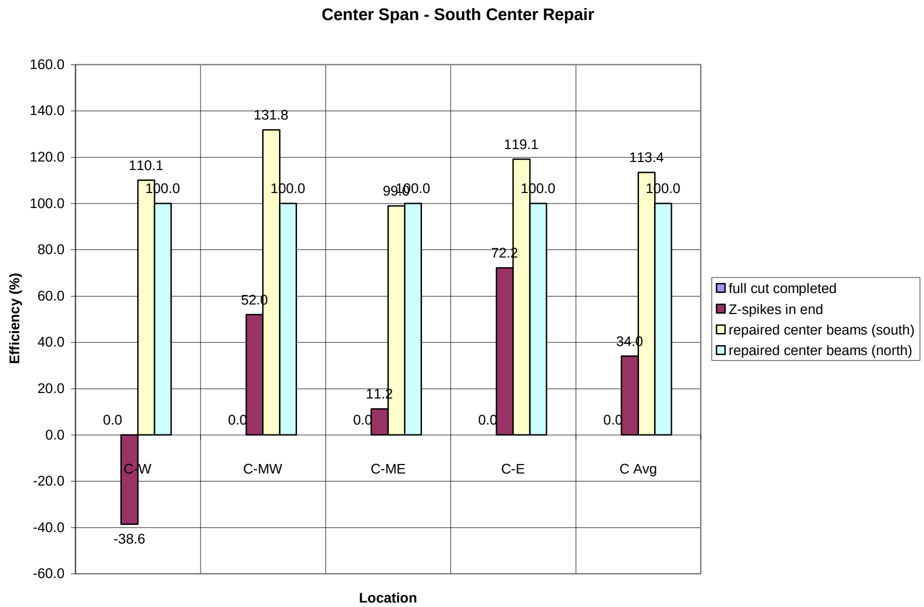

Figure 11: Efficiencies of the center span due to south end center repair (ST_i = "full cut completed" and ST_k = "repaired center beams (north)")

The efficiencies of the Z-spike insertion progression are shown in Figure 12. The "no damage" state was used as ST_k and the "full cut completed" state was used as ST_i in calculating efficiency from Equation 2. It was evident that the installation of Z-spikes to repair the cut increased the effective stiffness. On average, the last set of Z-spikes (inserted at the quarter point of the damage) had more effect than either of the other two sets. On average, the second set (inserted at the three-quarters point of the damage) had less effect than the other two sets.

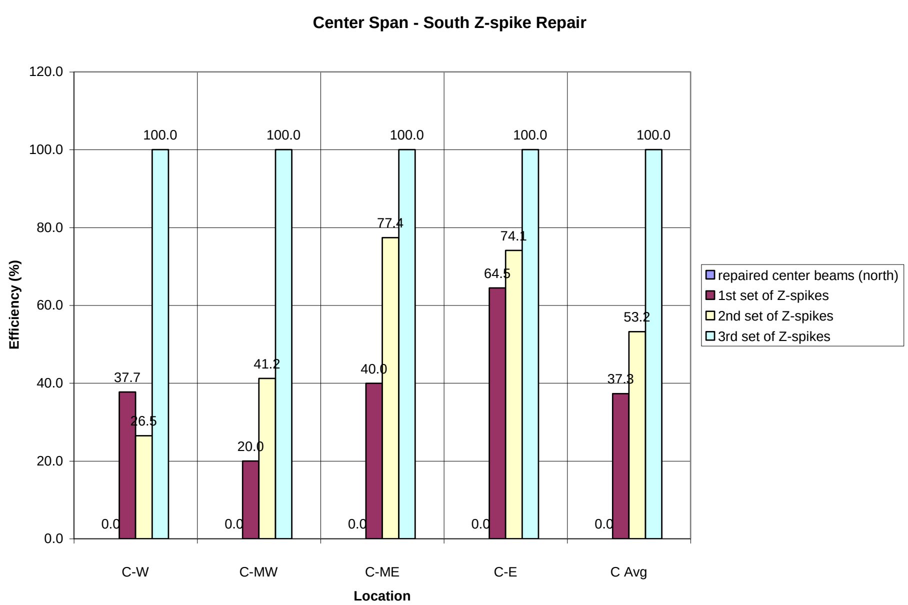

Figure 12: Efficiencies of the center span due to south end Z-spike repair (ST_i = "repaired center beams (north)" and ST_k = "3rd set of Z-spikes")

The efficiencies of the combination of the center repair and the Z-spike repair are shown in Figure 13. The "3rd set of Z-spikes" state was used as ST_k and the "full cut completed" state was used as ST_i in calculating efficiency from Equation 2. It was evident that each of the four stringers followed approximately the same behavior from state to state. The efficiency of all four stringers increased in the first and second states, then decreased or remained approximately the same in the third state, then increased again in the fourth, fifth, and sixth states.

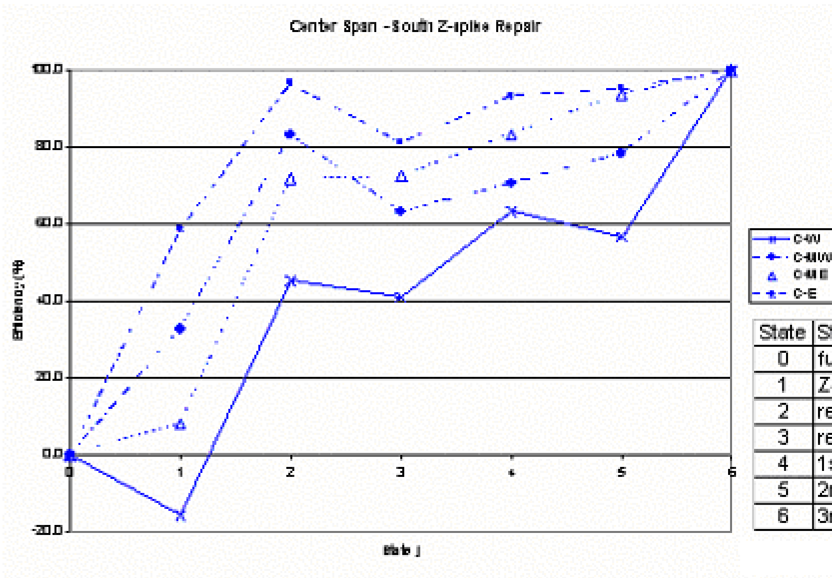

State	Stringer Condition
0	full cut completed
1	Z-spikes in end
2	repaired center beams (south)
3	repaired center beams (north)
4	1st set of Z-spikes
5	2nd set of Z-spikes
6	3rd set of Z-spikes

Figure 13: Efficiencies of the center span due to south end repair (ST_i = "full cut completed" and ST_k = "3rd set of Z-spikes")

Damage/Repair to North End

For the damage/repair in the north half of the center span of the beams, the stiffness and efficiency for each member in the center span were calculated before the damage, after the damage, and with each incremental addition of the five sets of Z-spikes. The patterns of changing measured ST of the center span due to the repair of the inflicted damage in the north end are shown graphically in Figure 14. The load-deflection data used to calculate the effective stiffness for the north end damage/repair can be found in Burgers et al. (2005).

From Figure 14 it is evident that the installation of Z-spikes increases the effective stiffness of the stringers in the center span. For the four stringers in the center span, the average effective stiffness was 8.72×10^3 kN-m^2 for the first set of Z-spikes, 8.99×10^3 kN-m^2 after adding the second set, 9.32×10^3 kN-m^2 after adding the third set, 9.57×10^3 kN-m^2 after adding the fourth set, and 9.80×10^3 kN-m^2 after adding the fifth set.

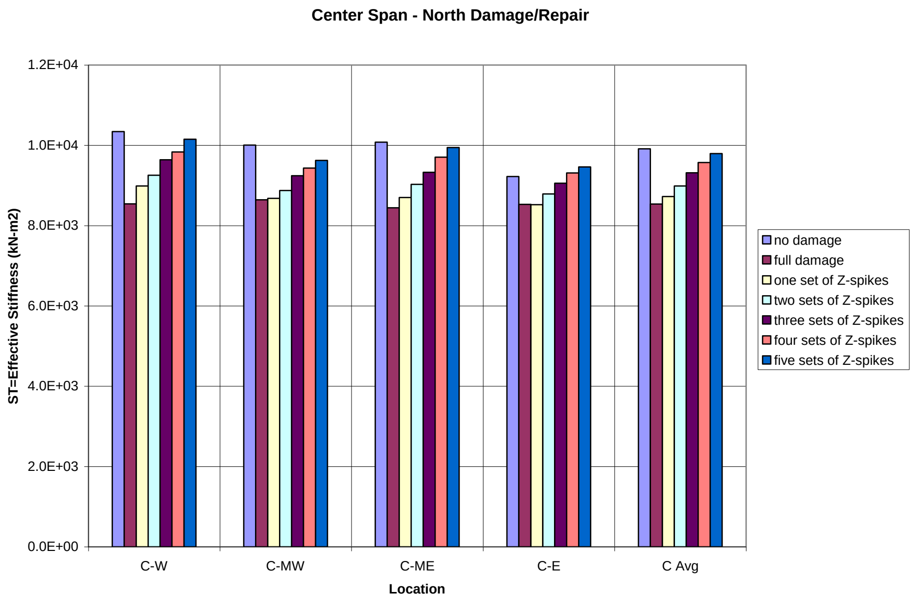

Figure 14: Effective stiffness of the center span due to north end damage/repair

The effective stiffness increases of the four stringers varied throughout the testing. For example, after the installation of the first set of Z-spikes, the effective stiffness values were 8.99 x 10^3 kN-m^2, 8.68 x 10^3 kN-m^2, 8.70 x 10^3 kN-m^2, and 8.52 x 10^3 kN-m^2 for the west, middle west, middle east, and east stringers, respectively. After the installation of the fifth set, the corresponding effective stiffness values were 10.2 x 10^3 kN-m^2, 9.62 x 10^3 kN-m^2, 9.95 x 10^3 kN-m^2, and 9.46 x 10^3 kN-m^2, respectively.

The efficiencies of the Z-spike repair are shown in Figure 15. The “no damage” state was used as ST_k and the “full damage” state was used as ST_i in calculating efficiency from Equation 2.

From Figure 15 it is evident that the installation of Z-spikes increases the efficiency of the members in the center span. For the four stringers in the center span, the average efficiency was 13.4% for the first set of Z-spikes, 32.6% after adding the second set, 56.7% after adding the third set, 75.3% after adding the fourth set, and 91.6% after adding the fifth set. After five sets of Z-spikes, the effective stiffness was nearly the same magnitude as that of the members before they experienced damage due to the cut. One value (C-E) actually exceeded the original effective stiffness, that is, the efficiency was 134%. The unexpected damage was the most severe in this member, thus it is believed that the effective stiffness exceeded the original effective stiffness because the addition of Z-spikes was repairing the cut that was made in the north half plus part of the unexpected damage that occurred in the south half.

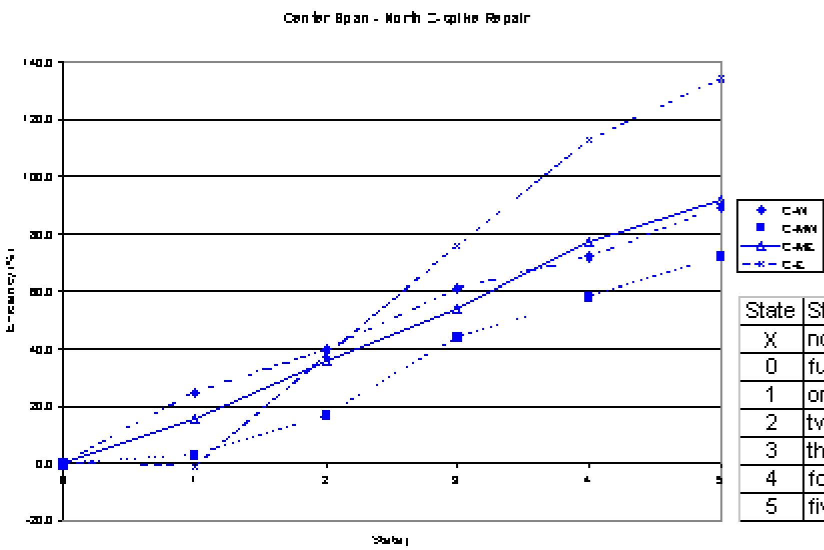

State	Stringer Condition
X	no damage
0	full damage
1	one set of Z-spikes
2	two sets of Z-spikes
3	three sets of Z-spikes
4	four sets of Z-spikes
5	five sets of Z-spikes

Figure 15: Efficiency of the center span due to north end damage/repair
(ST_i = "full cut completed" and ST_k = "no damage")

The increase in effective stiffness of the four members varied throughout the testing. For example, after the installation of the first set of Z-spikes, the increases in effective stiffness were 24.8%, 2.7%, 15.8%, and -1.2%, for the west, middle west, middle east, and east stringers, respectively. After the installation of the fifth set, the corresponding increases in effective stiffness were 89.5%, 72.1%, 92.0%, and 134.4%, respectively.

Conclusions

By not drilling a hole through the complete depth of the stringers, no epoxy was pushed out the bottom and all was used. It was visually observed on the outside stringers that beads of epoxy had penetrated from the drilled hole through the wood fibers. It was concluded that the epoxy was entering the voids in the wood fibers, which was an added contribution to the stiffening of the stringer.

The use of vertically-oriented Z-spikes significantly improves the effective stiffness of full-scale timber stringers in a bridge chord specimen. The use of five sets of Z-spikes in the north half of the center span averaged 91.6% recovery of the effective stiffness lost due to intentional damage from a cut at mid-depth. The high and low effective stiffness recoveries were 134.4% and 72.1%.

The results of this large-scale testing were similar to that measured by Radford et al. (2000–2003) and Schilling et al. (2004) at smaller scales. As each set of shear spikes was inserted in the laboratory specimen, the effective stiffness increased. The 91.6% average effective stiffness recovery due to the use of shear spikes to repair the north end damage was comparable to the effective 100% repair measured by Radford et al. (2000–2003) when 2x4s were split and repaired.

The Z-spikes developed significant interlayer shear transfer between the top and bottom layers in the intentionally damaged area.

The dense use of Z-spikes in the center third of the center span to repair the region of unexpected damage (cracking under load) increased the effective stiffness for each of the four stringers. But since there was not enough data to determine how much the effective stiffness changed due to the unexpected damage, it was not possible to quantify to what degree this unexpected damage was repaired.

Acknowledgments

This study was conducted using funds provided by the U.S. Department of Transportation to the Mountain Plains Consortium (MPC), via the University Transportation Centers Programs. Colorado State University is a member of the MPC, and the work was done at its Structural Engineering Laboratory. Students Steve Babcock, Misty Butler, Charles Manu, Rob Suarez, Elliot De Jongh, and Karl Wolfswinkel assisted with the physical testing. The contents of this paper reflect the views of the authors, who are responsible for the facts and the accuracy of the information presented. The U.S. Government assumes no liabilities for the contents or use thereof.

References

1. American Railway Engineering Association, “1995 Manual for Railway Engineering,” AREA, Washington, D.C.
2. Barbero, E.’ Davalos, J. & Munipalle, U. (1994). Bond strength of FRP-Wood Interface. *Journal of Reinforced Plastics and Composites*, *13*, 835-854.
3. Bohannan, B. (1962). Prestressing wood members. *Forest Products Journal, 12 (12)*. 596-602.
4. Bulleit, W.M. (1984). Reinforcement of Wood Materials: A Review. *Wood and Fiber Science*, *16 (3)*, 391-397.
5. Burgers, T. (2005). Composite Repair of Full-Scale Timber Bridge Chord Members through the Process of Shear Spiking. Masters Thesis, Colorado State University, Fort Collins, CO.
6. Burgers, T., Gutkowski, R.M.; Radford, D., and Balogh, J (2005). Composite Repair of Full-Scale Timber Bridge Chord Members through the Process of Shear Spiking. Mountain Plains Consortium, Report No. 05-173, North Dakota State University, Fargo, ND.
7. Cox, B.N. (1999). Mechanisms and Models for Delamination in the Presence of Through Thickness Reinforcement. Proceeding ICCM-12, Paris, July 1999.
8. Davalos, J.F., Qiao, P., and Trimble, B.S. (2000). Fiber-Reinforced Composite and Wood Bonded Interfaces: Part 1. Durability and Shear Strength. *Journal of Composite Technology and Research*, *22*, 224-231.
9. Davalos, J.F., Qiao, P., and Trimble, B.S. (2000). Fiber-Reinforced Composite and Wood Bonded Interfaces: Part 2. Fracture. *Journal of CompositeTechnology and Research, 22,* 232-240.
10. Davalos, J.F., Zipfel, M.G., and Qiao, P. (1999). Feasibility Study of Prototype GFRP Reinforced Wood Railroad Crosstie. *Journal of Composites for Construction*, *3*, 92-99.

11. Doyle, K.R., Gutkowski, R.M., Criswell, M.E., Pellicane, P.J, and Balogh, J. (2000). Laboratory Tests and Analysis of Full-Scale Open-Deck Timber Trestle Railroad Bridge Chords. Structural Research Report No. 82, Colorado State University.
12. GangaRao, H.V.S, Sonti, S.S., and Superfesky, M.C. (1996). Static Response of Wood Crossties Reinforced with Composite Fabrics. International Society of the Advancement of Materials and Process Engineering Symposium and Exhibition. Volume 41, 1291-1303.
13. Gentile, C., Svecova, D., and Rizkalla, F. (2002). Timber Beams Strengthened with GFRP Bars: Development and Applications. *Journal of Composites for Construction*, *6*, 11-20.
14. Gutkowski, R.M., and Balogh, J. (2001). Refined Load Tests and Analysis of a Timber Trestle Railroad Bridge Specimen. Proceedings 9th International Conference and Exhibition in Structural Faults and Repair—2001, ASCE, London, UK.
15. Gutkowski, R.M., Doyle, K.R., and Balogh, J. (2002). Full-Scale Laboratory Testing of a Timber Trestle Railroad Bridge Chord (Phase 1). Mountain Plains Consortium, Report No. 02-139, North Dakota Sate University, Fargo, ND.
16. Gutkowski, R.M., Peterson, M.; Robinson, G.C., Uppal, U., Oliva-Maal, D., and Otter, D. (1999). Field Studies of Timber Railroad Bridges. Association of American Railroads, Transportation Technology Center, Inc, Report No. R-933, Pueblo, CO.
17. Gutkowski, R.M., Shigidi, A.S.; Tran, A.V., Uppal, U., and Otter, D.E. (2002). Field Study of a Strengthened Timber Railroad Bridge. Association of American Railroads, Transportation Technology Center, Inc. Report No. R-956.
18. Gutkowski, R.M., Shigidi, A.M.T., Tran A.V., and Peterson, M. (2001). Field Studies of a Strengthened Timber Railway Bridge. Presented and written in Transportation Research Record No. 1770 Design of Structures 2001. *Journal of the Transportation Research Board,* National Research Council, Washington D.C.
19. InterCad Kft, (2003) Axis VM Version 7 User's Manual. Budapest Hungary.
20. Johns, K.C.; Lacroix, S. (2000). Composite Reinforcement of Timber in Bending. *Canadian Journal of Civil Engineering*, *27*, 899-906.
21. Lantos, G. (1964). Reinforced and Post-tensioned Glue-laminated Beams under Development at TRADA Labs. *Civil Engineering and Public Works Review*, London *59*, 690.
22. Liberty Pultrusions. (2004). Pultruded Rod Technical Data,.
23. Oomen, G., and Sweeney, R.A.P. (1996). Application of Modern Technologies in Railway Bridge Infrastructure Management and Decision Making. NATO ASI Series, Partnership Sub Series 2, Environment. Volume 5, 339-346. (need publisher), Springs Verlag
24. Peterson, J.L. (1965). Wood Beams Prestressed with Bonded Tension Elements. *ASCE Journal Structural Division 91(ST1)*, 103-119.
25. Pault, J.D. (1977). Composite Action in Glulam Timber Bridge Systems. Master of Science Thesis, Colorado State University, Fort Collins, Colorado.
26. Radford, D., Gutkowski, R., Van Goethem, D., and Peterson, M. (2003). Pultruded composite shear spike for repair of timber members. STREMAH 2003, Eighth International Conference on Structural Studies, Repairs and Maintenance of Heritage Architecture, Halkidiki, Greece, Wessex Institute of Technology, UK, 737-750.
27. Radford, D.W., Peterson, M.L. & VanGoethem, D. (2000). Composite Repair of Timber Structures. Mountain Plains Consortium, Report No. 00-112, North Dakota State University, Fargo, ND.

28. Radford, D., Van Goethem, D.; Gutkowski, R.M., and Peterson, M.L. (2001). Composite repair of Timber Bridges. Proceedings 9th International Conference and Exhibition in Structural Faults and Repair—2001, ASCE, London, UK.
29. Radford, D., Van Goethem, D.; Gutkowski, R.M., and Peterson, M.L. (2002). Composite Repair of Timber Structures. *Construction and Building Materials*, Elsevier Publications, 16, 417-425, North Dakota State University, Fargo, ND.
30. Schilling, T.J., Gutkowski, R.M. and Radford, D. (2004). Composite Repair of Railroad Crossties through the Process of Shear Spiking. Mountain Plains Consortium, Report No. 04-163.
31. Sliker, A. (1962). Reinforced Wood Laminated Beams. *Forest Products Journal*, *12 (2)*, 91-96.
32. Steves, C.A. and Fleck, N.A. (1999). In-Plaece Properties of CFRP Laminates Containing Through-Thickness Reinforcing Rods (Z-pins). Proceeding ICCM-12, Paris.
33. Uppal, U. and Otter, D.E. (1998). Methodologies for Strengthening and Extending Life of Timber Railroad Bridges. Association of American Railroads, Transportation Technology Center, Inc, Report No. R-92, Pueblo CO.